Wind turbine wake: bridging the gap between large eddy simulations and wind tunnel experiments

Wind turbine wake: bridging the gap between large eddy simulations and wind tunnel experiments

E. Gillyns[1,2], S. Buckingham[1], J. van Beeck[1] and G. Winckelmans[2]

[1] von Karman Institute for Fluid Dynamics, 1640 Sint-Genesius-Rode, Belgium
[2] Institute of Mechanics, Materials and Civil Engineering (IMMC), Université catholique de Louvain (UCLouvain), 1348 Louvain-la-Neuve, Belgium

E-mail: emmanuel.gillyns@vki.ac.be

Abstract. The wind industry has experienced rapid growth over the past two decades and wind energy is expected to continue leading the way in the global energy transition. Additional wind farms are expected to be installed in the coming years, both offshore and onshore. In view of exploiting any suitable terrain, an increased number of turbines are installed in close proximity to existing structures, thus exposing these to the wake turbulence. For instance, electrical cables are regularly exposed to those higher levels of turbulence compared to design loads, potentially leading to premature failure of the power line. It is hence essential to have a good understanding of these phenomena to be able to mitigate their effects. Scale-resolving investigations using Large Eddy Simulation (LES) can provide insight into site-specific loading conditions when combined with an Actuator Line Model (ALM), which reproduces the reaction force of each blade on the flow while still using a relatively coarse grid. The ALM used in this framework was newly-implemented in the spectral element code Nek5000, a highly efficient code with reduced cost per degree of freedom and exponentially fast convergence. The present work aims to bridge the gap between LES and a well controlled wind tunnel test of a scaled wind turbine, for validation purposes.

First, a small scale wind turbine of diameter 80 cm is designed and tested in a well controlled wind tunnel environment. Experimental data are gathered ahead of it and in its wake, and the mean velocity and turbulence intensity profiles are presented.

Although blockage effects are kept to a minimum, they will be accounted for in the simulations to ensure a better comparison with the measurements. In this work, we focus on a single inflow velocity field and on a fixed rotation speed.

Simulating the produced wake using LES combined with ALM remains challenging as the results are very sensitive to the turbulent inflow conditions and also to the airfoil aerodynamics used in the ALM. In the experiment, the incoming profile is also that of a developing flow and accurately reproducing its main characteristics is required for proper inflow to the LES. A "Recycle and Rescale Method" (R2M) will be hence be used as it is well suited for such case. The method will allow for the relevant turbulent boundary layer structures to be properly reproduced numerically, hence ensuring that the wind turbine is exposed to similar inflow conditions than in the experiment.

With the developed framework, the comparison between the wake produced in the experiment and that obtained using LES with ALM will provide the necessary data to further adjust the parameter and grid size used for the LES and the polar model used in the ALM.

Keywords: Actuator Line Model, wind turbine wake, LES, spectral element, Nek5000, experimental wind turbine, small-scale wind turbine, wind tunnel test, turbulent wake.

1. Introduction

With the current trend to the green energy transition, wind power is the leading renewable energy source in Belgium with 12.5 % of the electricity produced in 2022 coming from wind turbines. This number is still increasing, and more wind turbines will be installed, both onshore and offshore.

Wind turbine wakes extend far downstream and correspond to a highly turbulent flow that can have a significant impact on any encountered structure: another other wind turbine, a building, but also electrical cables. Indeed, the large dynamic displacement of cables caused by wake turbulence has be found to lead to significant damages, and even to premature failure.

Numerical simulation can help reveal the driving mechanisms associated to wake turbulence, and also support the development of mitigation strategies. For that, Large Eddy Simulation (LES) can be used as it allows to capture the dynamics of the relevant turbulent scales of the flow, down to the scale of the near tip blade chord. The blades themselves are not resolved by the simulation; instead their effect on the flow is represented using an Actuator Line Model (ALM).

The present paper aims at developing a coherent framework to allow for a detailed comparison between the experimental data collected in a wind tunnel with a scaled wind turbine and the results of LES with ALM run under the same conditions (i.e., same inflow velocity field, blockage, loading distribution over the blades, thrust and power coefficients of the wind turbine).

2. Experimental setup

2.1. Wind tunnel

The results from a numerical simulation should be compared to those of an equivalent experiment in a well controlled environment (such as a wind tunnel). This also requires to be able to reproduce the experimental environment numerically, so as to be able to perform a proper validation.

The first thing we consider is the spatial resolution: a fairly large wind turbine model is sought for as it will allow for a better spatial resolution of the measurements. This in turn requires a large wind tunnel as the blockage effects should be kept to a minimum for the results to be representative of a full scale wind turbine.

The wind tunnel used here is the low speed L1-B at the von Karman Institute. It is a closed-loop wind tunnel with test section dimensions of 3 m in width, 2 m in height, and a length of $\simeq$20 m. A schematic of the test section is presented in Figure 1.

The test section is equipped with a roughened floor to allow the growth of a turbulent boundary layer similar to the lower part of an atmospheric boundary layer (ABL) in neutral conditions. The flow can be adjusted from 1 to 50 m/s; the present case will focus on a value of $\simeq$6.5 m/s. This is such that the rotational speed of the wind turbine remains safe to operate.

The wind turbine, detailed in the next section, has a diameter of ø80 cm, and a hub height of 61 cm. It is placed at the beginning of a turntable, where the height of the boundary layer has reached the height of the half-channel (1 m), and where the flow is no longer developing significantly. This location constitutes a trade-off between putting it as far downstream to have a fully developed incoming profile, and as far upstream to allow for the measurement of the wake. As shown in Figure 1, a probe displacement system has been added to measure at three locations (labeled (1), (2) and (3)) using hot wire anemometry. The probe is secured using a pole, displaced in the test section with minimal intrusiveness, as shown in Figure 2a. Hot wire anemometry is used to capture the mean flow velocity as well as the fluctuations.

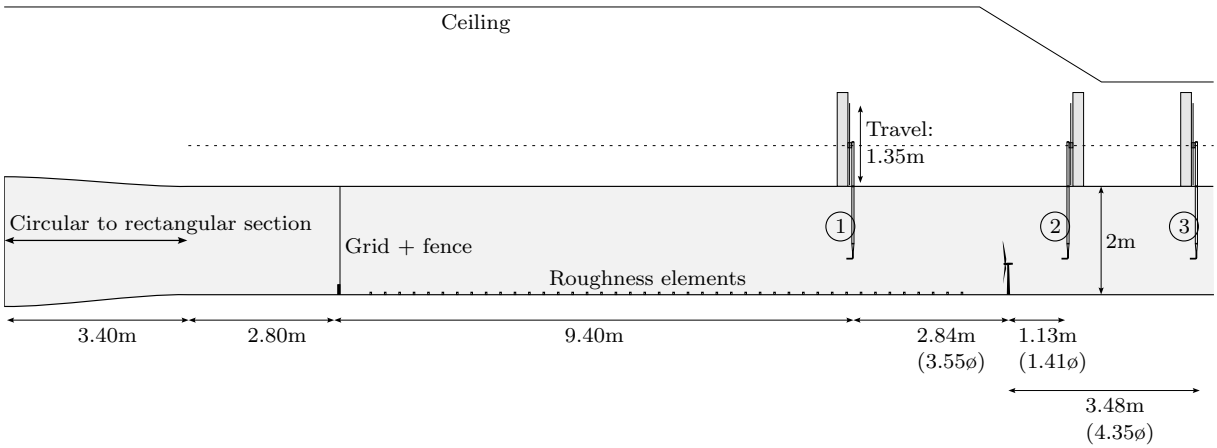

Figure 1: Test section for the L1-B wind tunnel.

2.2. Wind turbine model

The wind turbine model has been developed for providing a validation case for LES with ALM which reproduces the wake of a wind turbine as close as 1 wind turbine diameter downstream (1D). It is therefore important to have a nacelle as compact as the full scale wind turbines in relative terms.

(a) Wind turbine and hot wire setup in the L1-B test section

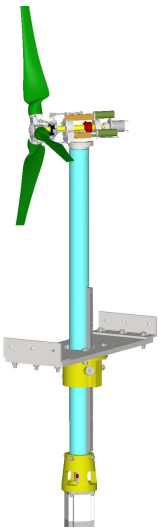

(b) CAD of the wind turbine

Figure 2: Wind turbine model installed in the L1-B test section and its CAD.

The first parameter, defining the diameter of the rotor, is the blockage effect in the wind tunnel, which cannot be avoided but should be minimized. The interaction with the ground is desired, therefore this region should be omitted from the blockage calculation. According to [1], the blockage ratio $B = \frac{swept\ area}{wind\ tunnel\ area}$ should be <10 %, and the minimum distance to a wall should be $> 1D$. With those constrain, the resulting wind turbine is 80 cm in diameter, at a hub height of 61 cm. The blockage, excluding the region below hub height, is 6.0 %, with a clearance to the top wall of 1.0 m.

We also wish to produce a wake whose statistics are independent of the Reynolds number, as

described in [2]. According to this reference, this independence start at $Re \approx 9.3 \times 10^4$ (with Re based on the rotor diameter and free steam velocity). The present wind turbine model operates at $Re \geq 35 \times 10^4$, which is well above that recommendation.

The support of the wind turbine allows yaw control. The nacelle has been kept to a minimal size, in an attempt to obtain a realistic ratio to the swept diameter. Components inside the nacelle are kept within a diameter of ø8 cm, thus 10 % of the swept diameter. It contains a swash plate controlled by three electric motors allowing the pitch control, both collective and cyclic. Additionally, to allow the placement of sensors on/in the blade (such as strain gauge at the root and pressure sensor inside the blade), a slip ring is used to transfer the signals from the rotating frame to the stationary one. As those elements occupy space in the nacelle, the generator is placed under the wind tunnel, the aerodynamic power being transmitted through a set of spiral bevel gears. The total length of the nacelle, from the base of the blade support to the furthest part downstream, is 231 mm which is approximately 3 times the nacelle diameter.

With the generator placed under the wind tunnel, a rack and pinion are used to change the height of the wind turbine inside the test section.

The blades have been 3D printed using the plastic PLA+, a variation of PLA with added material making the resulting part more ductile. The ductility of the material allows the blade to flex under load without breaking. It is attached to the wind turbine using a cylindrical hole at the base of the blade, in which a steel rod is inserted, which is then attached to the pitch control mechanism with tight manufacturing tolerance. The airfoil used for the blades is the SD7037-092-88, a low Reynolds airfoil which is suited for such small wind turbine. This airfoil shape is used for the whole blade. Compared to airfoil used in large wind turbine, it is more slender to avoid detachment of the boundary layer at the lower Reynolds numbers. The twist angle and chord distribution of the blades have been designed using a classical BEM approach. A second iteration of the blade design could improve the total power extraction, mostly to improve the region close to the blade root, but the current design can already serve as a validation case, as the same parameters will be used for the ALM model.

Because this wind turbine is being used for experiments regarding the wake, the electrical power generated is dissipated in an electrical resistance. The control strategy for regulating the rotational speed is to vary the load on the generator by connecting more/less electrical resistances on the generator, using a set of relays. Ten resistances are used, each having a resistance double of the previous one. This results in a 10-bit binary code for the load of the wind turbine, which provides 1024 possibles load values; hence an almost continuous set of loadings. The 3 phase alternating current (AC) generator is converted to direct current (DC) using a full bridge rectifier, before being connected to the load. This ensures a balanced load on the three phases at all times, and it eases the control equipment. An encoder is attached to the generator to obtain the rotational speed of the wind turbine, connected to an Arduino, which also controls the relays to act on the load.

In the scope of this study, the wind turbine is operated at constant speed, and with the same inlet velocity profile. One could assume that the load can be set manually once to obtain the desired rotational speed during the tests. However, as the resistances dissipate a significant amount of energy, the temperature changes throughout the experiment. The electrical resistance being proportional to the temperature, there is then a significant drift over time, and the load needs to be adjusted dynamically to maintain the rotational speed constant. For this, a Proportional-Integral (PI) controller is used on the Arduino. It is a Single-Input Single-Output (SISO) controller with the rotational speed as input, and the set of relays loading the generator with resistances as output. The parameters of this controller were adjusted experimentally by linearization around the desired operating point, with effective results.

The rotational speed was defined arbitrarily to 700 RPM (which is a Tip Speed Ratio TSR of 4.6, where the optimum of the current design is $\simeq 5$). This parameter does not have to match

the optimum, and can be reproduced in LES easily.

3. Experimental measurements

Measuring the wake is performed using hot wire anemometry. This technique provides high frequency response, hence it is able to measure the turbulent fluctuations. The downside of this methodology is the aging of the wire during its operation, which requires to re-calibrate it periodically. Multiple methodologies were explored for this calibration, but only the selected method is presented here.

3.1. Calibrations

First, a pressure transducer compensated in temperature has been calibrated using both a water manometer and a reference pressure calibrator, see Figure 3a, with the combination of them reducing the total uncertainties. This calibration has been repeated over one week, and no drift in time was observed, giving good confidence in the measurements. This pressure transducer is then used to measure the difference in pressure between a pitot tube placed in the center of the test section (at 982 mm from the bottom wall) and a static pressure tap on the wall. Assuming incompressibility, the Bernoulli equation is used to convert the difference of pressure into the local flow velocity. This operation is performed at both locations (1) and (2), where the hot wire will be measuring the profile.

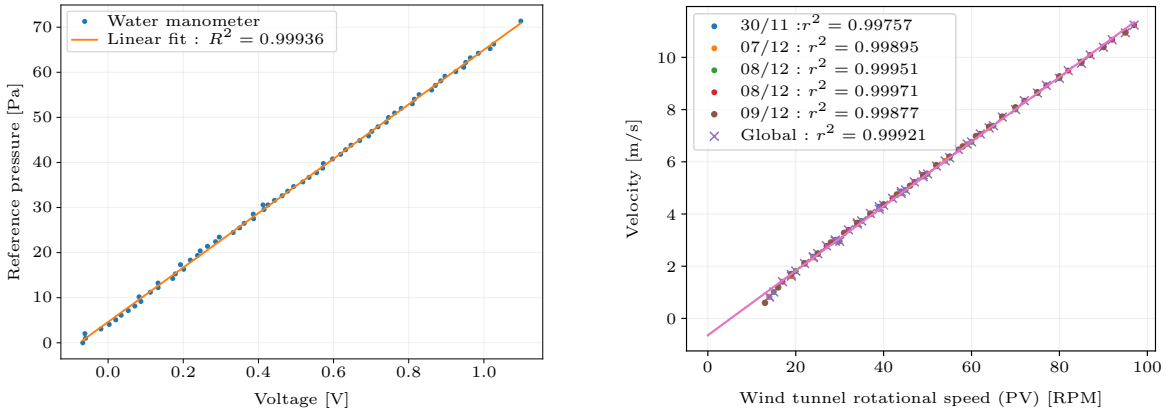

(a) Pressure transducer calibration. (b) Wind tunnel calibration.

Figure 3: Calibration method for the reference velocity.

Next, the wind tunnel is set at multiple velocities, relating the rotational speed of the motor to the local flow velocity at the center of the channel. This relationship is shown in Figure 3b. This step has been repeated over two weeks, with excellent repeatability, giving good confidence in the methodology; then repeated at both locations (1) and (2).

Finally, the pitot tube was replaced with the hot wire mounted on an automated displacement system. Calibration of the hot wire was performed periodically before and after each set of measurements, with a time between calibration ranging from 1 to 1.5 hours. All calibrations curves are shown in Figure 4. It is seen that the curves differ slightly from each other, showing that the calibrations were frequent enough to minimize uncertainties. Overall, one can observe a trend for the curves to move towards the left, as the wire ages over time.

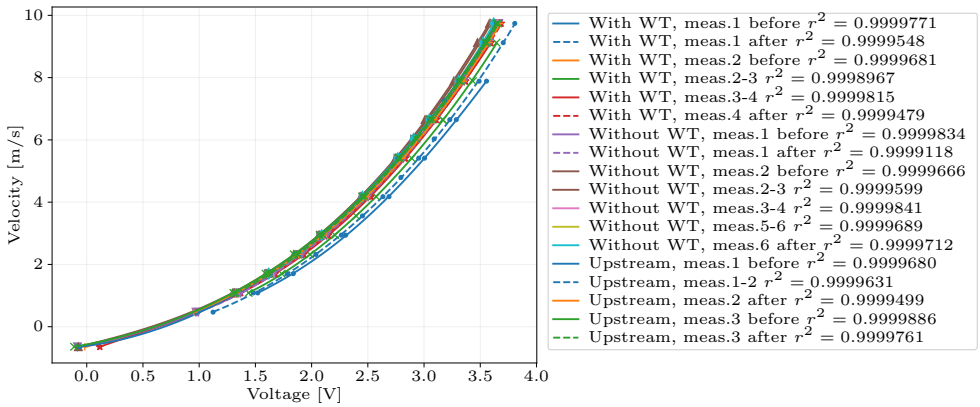

Figure 4: Hot wire calibrations.

3.2. Measurements

So far, measurements were performed at locations (1) and (2) of Figure 1. They will also be performed at location (3) in the future. We see that the height of the test section (2 m) is bigger than the travel of the hot wire traverse system. Measuring over the entire height of the test section has to be done in two parts, with an overlap region.

Location (1) is ideally positioned to be sufficiently upstream from the wind turbine such that it is unaffected by its presence, and sufficiently downstream in the test section to capture the effect of the roughened bottom wall. This profile is also required to impose the inlet in the numerical simulation. The measurement was done in two parts, with significant overlap, and measurements repeated over two days. The overlap is observed between 800 mm and 1200 mm, with a good repeatability. Figure 5 shows the resulting profile, with measurement 1 taken on

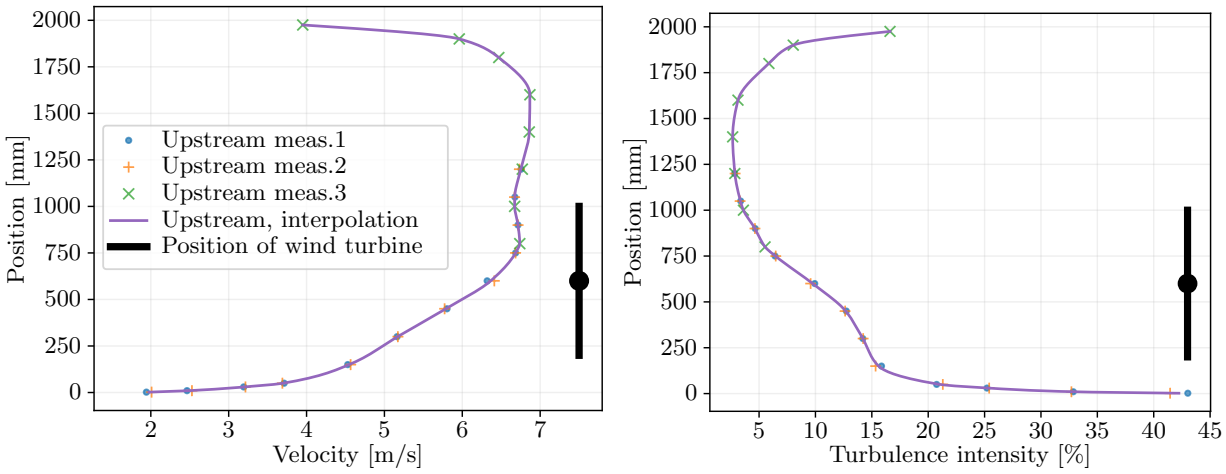

(a) Mean velocity profile.

(b) Turbulence intensity profile.

Figure 5: Measurements at location 1.

one day, and measurements 2 and 3 taken on the next day to ensure repeatability. The profile is overall a developing profile, with the bottom boundary layer height being well-developed (reaching close to the half channel height), while the top boundary layer is much thinner due to the smooth wall. The resolution at the top is not as good as that at the bottom, as this region affects very little the wind turbine and only serves to capture the blockage effect of the wind

tunnel. The uppermost point is also not as close to the wall as the lowermost point: this is due to the shape of the probe, designed for measuring the boundary layer at the bottom.

The turbulence intensity profile measured is given in Figure 5b. This was measured with a hot wire facing the flow horizontally, meaning that it is sensitive to velocity fluctuations in the streamwise and vertical direction (without differentiation), not to the spanwise direction. From the measured signal of the hot wire, the calibration is applied, then its standard deviation is divided by the local mean velocity (shown in Figure 5a) to obtain the turbulence intensity.

Measurements at location (2) were made for both cases, with and without the wind turbine, and are presented in Figure 6. For each case, the profiles were measured on one day, and repeated on the next day to ensure repeatability, and also add resolution in the regions of interest (the measurement 1 was done on the first day, all others were done on the next day). Each reported value uses its own calibration curve, before and after the measurement, with a maximum time of 1.5 h between calibrations.

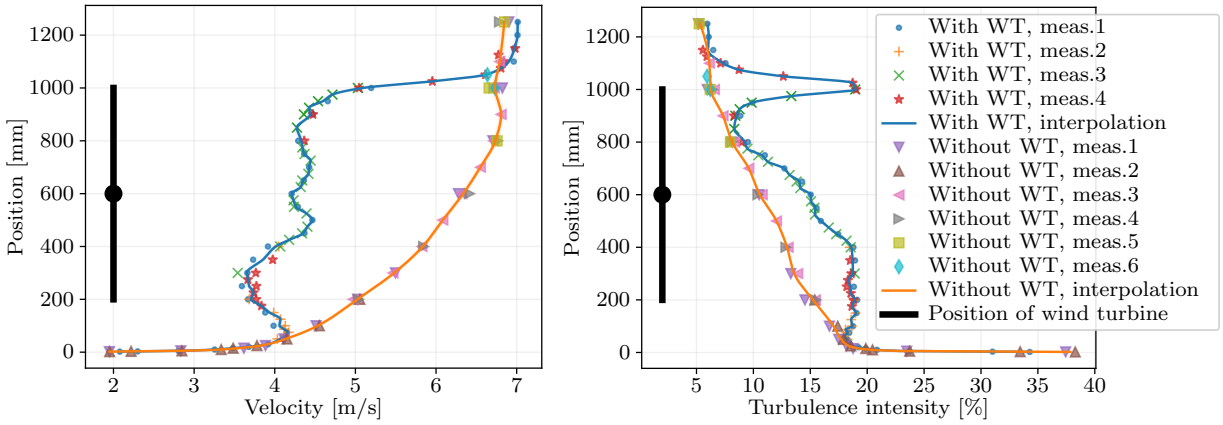

(a) Mean velocity profile.

(b) Turbulence intensity profile.

Figure 6: Measurements at location 2, with and without wind turbine.

The profile without the wind turbine (orange curve from Figure 6) shows a boundary layer height almost reaching the top height of the wind turbine. This depicts that the wind turbine will be subjected to a flow similar to that of an Atmospheric Boundary Layer (ABL) and which indeed encompasses the whole wind turbine. The profile also shows an inflexion point at about 1000 mm, where the bottom boundary layer meets the upper core flow. Measurements at this location were repeated multiple times to ensure that this is not an outlier.

Regarding the flow extraction from the wind turbine, the velocity deficit observed between the two curves shows that the wind turbine indeed extracts energy from the flow. The thrust coefficient is estimated using the two mean velocity profiles (with and without the wind turbine) measured at location (2); which leads to $C_t \simeq 0.46$. For that, the velocity is considered over a disk centered on the wind turbine axis and also slightly enlarged in diameter (to account for the expansion of the wake between the wind turbine location and location (2)). It is assumed homogeneous spanwise. The thrust available in each flow is estimated as $T = \frac{\rho}{2} \sum_i v_i^2 \cdot (w_i \Delta h)$ where ρ is the air density in the test section, v_i is the measured velocity at height i, w_i is the width of the strip associated to the disk at that height and h is the spacing used to discretize the strips. The difference between the two values of T is then used to estimate C_t.

Regarding the power coefficient, the losses between the aerodynamic power at the shaft and the electrical power are not yet quantified; they can only be roughly estimated. Measuring the electrical power of the 3-phase generator is done by measuring the line voltage and current,

before the conversion to DC and the load resistances; it is obtained as 18.2 W. If we ignore all losses, the electrical power coefficient is $C_p \simeq 0.25$ (compared to a theoretical designed value of $C_p \simeq 0.37$ at this TSR). The generator efficiency at such low rotational speed typically drops to $\simeq$75 %. An additional efficiency of $\simeq$90 % being applied to account for the bearings and the gears between the two shafts, the estimated aerodynamic power is $\simeq$27.0 W, corresponding to $C_p \simeq 0.36$.

It can be noted that the presence of the wind turbine accelerates the flow in the top region, as seen in Figure 6 (blue curve), which is due to the blockage effect and was expected. Nevertheless, this effect can be considered small, as it only accelerates the flow by $\simeq 3\,\%$ locally.

Overall the velocity deficit has an interesting shape, that was validated by the repeatability of the experiment. It can be observed that the velocity deficit is greater in the regions of the blade tip and nacelle, and lower in the region of the blade roots. The better extraction near the tip is expected, as this is where the blades were optimally designed. At the blade root, the mechanical link to the shaft forces the design to have a circular cross-section locally: this does not provide any lift contributing to the extraction of energy from the flow, but only drag. Progressing away from the blade root, there is a smooth transition to the airfoil shape which provides lift.

The velocity deficit in the wake of the nacelle is also significant, due to the drag associated with its blockage.

4. LES case methodology

As pointed out from numerous previous works, such as in [3], the wake behavior of a wind turbine is heavily influenced by the inlet velocity profile. The mean profile determines the local flow velocity on the wind turbine blades, affecting how much energy can be extracted for a chosen setup (rotation speed and blade pitch). On the other hand, the turbulence intensity of the inlet affects mostly the length of the wake, higher turbulence resulting in faster wake recovery and hence smaller wake length. It is therefore essential for a proper comparison between an experiment and a numerical simulation to reproduce the inlet with good accuracy. As such, even before introducing the wind turbine model and comparing the wake, it is essential to ensure a solid baseline case without the wind turbine, to ensure that the inlet profile used in the simulation matches well that measured in the experiment.

The case presented here is still work in progress, with results coming up in a near future. Nevertheless, the wind tunnel experiments presented above are also performed to support the development of a LES methodology that is consistent with these experiments. We here solely present the methodology as it is being pursued.

Experimentally, the top wall induces a noticeable blockage, which must also be reproduced numerically. The sides being much further away from the wind turbine, their effect is assumed to be negligible. The experimental profile is considered a developing profile, as the heights of the boundary layer between the top and the bottom do not coincide. To simulate such flow, a "Recycle and Rescale Method" (R2M) is used, which is suited for generating turbulent inflow conditions for LES. This method is able to produce realistic and self-consistent turbulence structures of a developing flow, as shown in [4]. It consists in sampling a plane downstream (referred as the recycling plane), and copying a scaled version of it at the inlet, repeated at each timestep.

The numerical methodology is split in two cases: the first one focuses on the reproducing the base flow of the test section without the wind turbine, ensuring that the LES profiles are matching fairly well those of the experiment. The second case will be based on the first one, with the added wind turbine modeled using an Actuator Line Model (ALM).

4.1. Simulation of the base flow

The numerical domain is composed of a box with the same height as that of the experiment, and a width large enough for a periodic boundary condition to be applied. Regarding the length, the box starts at the experiment location (1) and ends downstream after location (2) from Figure 1. This is the minimum size that will allow a fair comparison with the experiment at both locations, and includes a buffer zone at the end for the outflow boundary condition. The boundary conditions and the mesh used are shown in Figure 7. This results in a box of

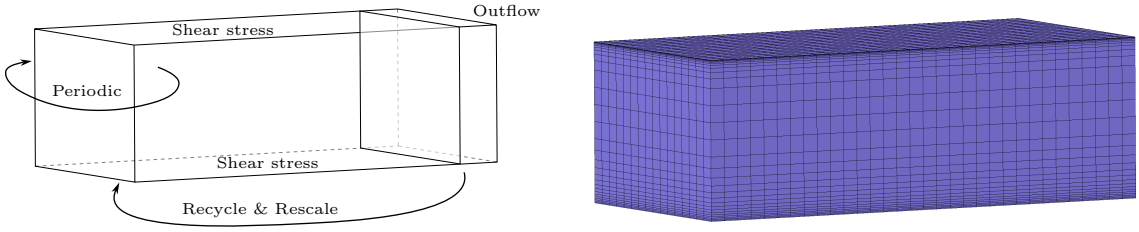

(a) Boundary conditions. (b) Mesh.

Figure 7: LES with recycle and rescale, used for conditioning of the inlet profiles.

5 m streamwise, 2 m vertically, and 3 m spanwise. The mesh is constructed using a uniform distribution streamwise and spanwise, and is refined near the walls. Based on our previous work [5], we use the newly validated wall-modeled LES (wmLES) within a spectral element method for the wall boundary conditions.

The so-called recycling plane is taken at $x = 4.5$ m, far enough from the outlet such that its effect is negligible. Due to the nature of the spectral element method, Gibbs phenomena are appearing at the element boundaries when performing LES, especially for the resolved turbulent fluctuations, see [5]. The R2M is often used to scale the boundary layer height in a developing flow, by applying the scaling on the position of each point. Doing such in this framework where Gibbs phenomenon are observed at the element interface, would amplify those numerical errors by moving them to the center of an element, hence additional frequency content would appear in the flow. The scaling used here is therefore applied on the magnitude of each node, based on the ratio between the time-averaged recycling plane and the experimental profile.

Once the inlet mean profile is imposed, the remaining degree of freedom consist in adjusting the shear stress of the wall model, such that the mean profile at location (2) matches that of the experiment.

Regarding the turbulence intensity: the wall shear stress will most likely provide the correct turbulence level near the wall. However, the turbulence measured experimentally in the free stream away from the wall is not negligible, even in the region where the mean velocity profile is essentially flat. Since this could also affect the resulting wake, a set of added randomized forces will probably be necessary to perturb the flow locally in the recycling region; with their amplitude being tuned so as to match the turbulence level in the simulation to that of the experiment.

4.2. Simulation of flow with the wind turbine

Once the base flow LES matches sufficiently well that of the experiment without wind turbine, we consider the next case which includes the wind turbine, here modelled using the newly implemented Actuator Line Model (ALM). The domain is similar to the previous one, but it is extended downstream to capture the wake. The parameters of the ALM are based on the effective design of the wind turbine. This includes the polar data for lift and drag of the airfoil used, the chord and twist distributions of the blade, the pitch angle, and the rotational speed.

In order to capture properly the behavior from the wind turbine, the mesh is refined in the region of the wind turbine, to allow the forces from the ALM to be properly captured. An illustration of the resulting mesh is provided in Figure 8.

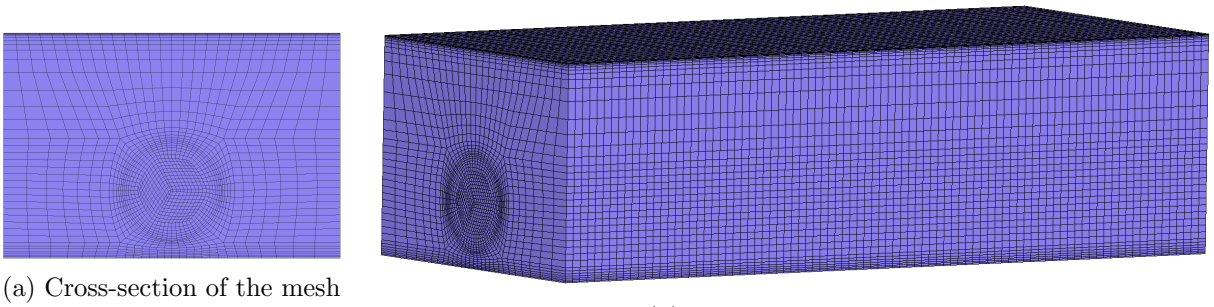

(a) Cross-section of the mesh

(b) Overview of the mesh

Figure 8: Mesh for the LES with the wind turbine.

With matching inlet mean velocity and turbulence intensity profiles from the previous case of the base flow (Section 4.1), the difference between the simulated wake and the experimental one shall be investigated, and any mismatch will be clearly identified.

Recall that it remains challenging to properly capture the near tip blade loading and the shedding of tip vortices when using ALM, as this is much influenced by the local resolution. This, in turn, can significantly influence the transition of the near wake to its turbulent state. The ALM in the near tip region will hence be more refined, so that the tip vortices are better captured and can better contribute to a transition to wake turbulence.

5. Conclusions

The presented work aims at reducing the gap between LES and wind tunnel experiments for wind turbine wake, and it is still work in progress. An experimental turbine was designed, built and used for future comparison with LES using an actuator line model. The estimated thrust and power coefficients are within the expected range, giving some confidence that the wake produced is representative of a wind turbine in normal operation.

Measurements have been performed at a location upstream of the wind turbine, to be imposed as inlet to the LES, and at a location downstream of it. The case without the wind turbine was also measured at both locations. The obtained results showed excellent repeatability and will be used to compare with future numerical results. The experimental profile at location (3) will also be measured in the future, bringing added data for the comparison with the LES.

The numerical simulation of this configuration is ongoing work. The pursued methodology was detailed and it is intrinsically linked to the way the experiments were designed and performed. The flow will be simulated in LES over the full height of the test section, and the numerical results will be used for a detailed comparison with those of the experiment. The differences between the two will also allow to fine-tune the parameters of the ALM representing the wind turbine.

Acknowledgments

This work is supported by a von Karman Institute PhD fellowship. The authors wish to acknowledge the work performed by the VKI technical staff, allowing the manufacturing of the wind turbine amongst other assistance. In addition, the staff in charge of 3D-printing at UCLouvain took charge of the printing of the blades, essential for the whole project.

The software used in the experiments, including the wind turbine controller, automation of the probe displacement and post-processing, has been built using free and open-source software; the authors thank the open source community, granting access to such powerful tools to anyone.

Finally, Emmanuel Gillyns would like to thank Tsvetelina Ivanova from the von Karman Institute for the help in the measurement process and for the valuable feedback.

References

[1] McTavish S, Feszty D and Nitzsche F 2013 *Wind Energy* **17** 1515–1529
[2] Chamorro L, Arndt R and Sotiropoulos F 2011 *Wind Energy* **15** 733–742
[3] Porté-Agel F, Bastankhah M and Shamsoddin S 2019 *Boundary-Layer Meteorology* **174** 1–59
[4] Xiao F, Dianat M and McGuirk J J 2016 *Flow, Turbulence and Combustion* **98** 663–695
[5] Gillyns E, Buckingham S and Winckelmans G 2022 *Flow, Turbulence and Combustion* **109** 1111–1131